



Contents lists available at ScienceDirect

Journal of Non-Newtonian Fluid Mechanics

journal homepage: www.elsevier.com/locate/jnnfm



Linear viscoelastic models Part I. Relaxation modulus and melt calibration

Tommi Borg^{a,*}, Esko J. Pääkkönen^b

^a TomCoat Oy, Koskisenkuja 11, 62500 Evijärvi, Finland

^b Tampere University of Technology, Laboratory of Plastics and Elastomer Technology, P.O. Box 589, 33101 Tampere, Finland

ARTICLE INFO

Article history:

Received 28 February 2008
Received in revised form 13 June 2008
Accepted 28 July 2008
Available online xxx

Keywords:

Polydispersity
Relaxation modulus
Melt calibration
Control theory
Inverse problem

ABSTRACT

Constitutive models for the linear viscoelasticity of polymers are presented for the relation between the relaxation modulus and the molecular weight distribution (MWD). We also compute the MWD from a simulated relaxation modulus curve by first obtaining the rheologically effective distribution (RED) as a function of time, and converting this into the MWD by *melt calibration*; that is, the relation between timescale and the molecular weight. This procedure has similarities with the widely used universal calibration with solved polymers. The main principles of our technique are applied here to familiar relaxation modulus data, for which we present two models: (1) an analytical model derived from control theory, which is known capable of modelling partially observed system and (2) a practical characteristic model for obtaining usable results. No relaxation time or spectrum procedures are used to model the process of linear viscoelastic relaxation. The use of relative calculations and melt calibration dispenses with the need to know the real chain structures such as branching and entangled chain dynamics, and the model remains useful for future investigations of polymer chain structures and dynamics, such as using tube theory.

© 2008 Elsevier B.V. All rights reserved.

1. Introduction

Determining the molecular weight distribution (MWD) or predicting viscoelastic properties requires the relaxation modulus or spectrum to be generated [1–21]. To overcome this *ill-posed problem*, several authors have recently used the double reptation model or the general mixing rule as analysed by Anderssen and Mead [22]. Thimm et al. [13] provided the first analytical relation for deriving the MWD from the modelled relaxation spectrum, even though this is impossible to measure directly.

Here we present two models for the relaxation modulus: The first is an *analytical* model based on the impulse function and control theory, which are well-known principles in mathematics, nuclear physics and signal control systems. Only two constants that depend on the polymer chemical structure are used, with no *ad hoc* tuning being necessary. The second, *characteristic* model uses the findings of the first model but is more practical and uses the measured time-dependent relaxation modulus, which is related to the MWD, $w(M)$. The computation strategy involves first finding a form of the MWD and relations using the rapidly

analysed characteristic model, and then confirming the obtained results using the analytical model, if necessary. Here we present the main principles of the new method with the help of the familiar relaxation modulus, $G(t)$. The basic criteria described above yield the procedure by which the MWD and broad-range curve of the linear viscoelastic relaxation modulus are simultaneously computed from simulated measurements of the relaxation modulus.

2. Theory

2.1. Relaxation modulus and structure information by the control theory

The modern control theory as applied to dynamic systems is used to model the relaxation modulus. One of the most important types of analysis is input–output modelling, in which the output data resulting from applying a test input to a system are analysed to yield useful information on cause–effect relationships and to reduce the model. Since this viewpoint is new in this field, we explain its basis here.

Molecular theories of rheology based on independent chain response (elastic dumb-bell, Rouse, Zimm) or pseudo-independent chain response (unmodified Doi-Edwards) can be used for predict-

* Corresponding author.

E-mail address: tommi.borg@tomcoat.com (T. Borg).

Nomenclature

\hat{G}_0	new fitted relaxation modulus at t_0
$G_c(t)$	characteristic relaxation modulus
Hf	conversion factor between M and t scales
Mf	structural value
$M(t)$	calibration curve for melts
P'	entanglement value
P''	Rouse value
R	ratio of effective distribution ranges
$w_i(t)$	effective fraction of the group of molecules
$w'(t), w'(\log t)$	rheologically effective distribution, (elastic) RED
$w''(t), w''(\log t)$	rheologically effective distribution, (viscous) RED''
$w'_c(t), w'_c(\log t)$	characteristic effective distribution, (elastic) RED

ing of the MWD according to Graessley [23] in *Polymeric Liquids and Networks: Dynamics and Rheology* (2008). For such systems, equations for viscosity, recoverable compliance and relaxation time in systems of arbitrary polydispersity can be obtained from the stress relaxation modulus, expressed as the sum of independent contributions. Thus,

$$G(t) = \sum w_i G_i(t). \tag{1}$$

in which w_i is the weight fraction of component i in the mixture, and $G_i(t)$ is the relaxation modulus for the monodisperse component.

We continue to develop the above principle further by converting weight fraction $w_i(M)$ as a function of molecular weight M to the function of time t or *effective fraction* $w'_i(t) = w_i(M)$ with the found relation between t and M discussed in Section 2.3. A similar conversion, but in the opposite direction, is widely used in wet chemical methods such as gel-permeation chromatography (GPC) tracing with time- or size-exclusion chromatography (SEC) for detecting the MWD.

Knowledge of the factors that influence the effective fraction, $w_i(t)$, is not essential, such as different types of chain dynamics, molecular friction and elasticity, reptation, primitive path fluctuations, constraint release, and other entangled and disentangled chain dynamics.

Chain types in the effective fraction $w_i(t)$ can conform to any linear short- or long-chain branched (SCB and LCB, respectively) structures, combs, networks, H-shapes with multiple arms, or any combinations of complete molecules or their segments. The final structure, molecular weight or construction of the statistical $w_i(t)$ fraction of a single molecule or groups of molecules is not important at this point—only its effects on viscoelasticity. Section 2.3 discusses the real sizes of the fractions. Now we rewrite Eq. (1) to get relaxation modulus functional as presented by Anderssen and Loy [24] for $G(t)$ as follows:

$$G(t) = \sum w_i(t) G_i(t). \tag{2}$$

We introduce the *rheologically effective distribution* (RED), $w(t)$, and impulse response $h(t)$ after induced stress at time t_0 . Relaxation modulus $G_i(t)$ in Eq. (2) has relation to a scaled product of $P' G_0 h(t_i)$, in which constants G_0 is zero modulus and P' is acting as a scaling factor. Thus we can rewrite Eq. (2) for $G(t)$ as

$$G(t) = G_0 P' \int_{-\infty}^t w(\tau) h(t - \tau) d\tau, \tag{3}$$

which can be explained and developed further by the control theory with the explanation starting from the basis.

We excite the system with a small stress induced by a small pulsed strain that is applied at time t_0 . Pulse response $y(t)$ is obtained from impulse response $h(t)$ and by sampling the active molecules in distribution $w(t)$ between some time interval:

$$y(t) = \int_{-\infty}^t w(\tau) h(t - \tau) d\tau. \tag{4}$$

This equation is the familiar linear formula used in control theory, which is known as a novel principle to adjust and rule one variable or function in a closed system and now in our case for MWD. Since the MWD function is normally a function of logarithmic variables, or here RED $w(\log t)$, we have to rewrite all variables and functions in Eq. (4) on a logarithmic scale. The logarithmic convolution (also known as the *scale convolution*) can be related to ordinary convolution by taking the logarithm of t , and since this is a linear operation it is commutative, associative, and distributive. Thus we can write $h(t) = t$ and $d\tau$ as $d(\log \tau)$.

Pulse response $y(\log t) = \log(G(t)/G_0)$ is a normalized relaxation modulus with a maximum value of zero on the logarithmic scale at t_0 . The value for zero relaxation modulus $G_0 = G(t_0)$ is obtained by fitting $G(t)$ to experimental measurements. We then obtain the complete relaxation formula in the case where a small and constant strain is induced:

$$\log \frac{G(t)}{G_0} = -P' \int_{-\infty}^{\log t} w(\log \tau) (\log t - \log \tau) d \log \tau. \tag{5}$$

With true distributions the normalized response on the logarithmic scale decreases, making the overall $G(t)$ a completely monotonically decreasing memory function, as analysed generally by Anderssen and Loy [25], and thus we have to add a negative sign to the right-hand side of Eq. (5). Entanglement constant P' is included since not all molecules in the distribution $w(t)$ related to MWD $w(M)$ will be active during the relaxation process due to intermolecule interactions by Matsuoka [26]. Also, the relation $(\Delta G(t)/\Delta w(t)) \propto P'$ at time step Δt depends on the baseline chemical molecular structure, chain types (SCB or LCB) and the average molecular weight. Therefore, it is necessary to adjust the normalized $w(\log t)$ distribution with the value of P' by feedback to obtain the fit for $G(t)$ as illustrated in Fig. 1, where the normalized distribution in Eq. (5) is

$$\int_{-\infty}^{\infty} w(\log t) d \log t = 1. \tag{6}$$

RED function $w(t)$ can be regarded as a GPC trace with a time-exclusion chromatography or SEC elugram function as a function of time. The largest molecules exit first from the GPC/SEC column, in a similar way to these molecules initially having greater relaxation effects with many entanglements and structural units during relaxation experiments or respectively orientating at the lowest frequency and shear rate.

To clarify the differences in the presented principle, we rewrite the simplified general form of classical integral equations with kernel $k(t, M)$ used in principle by [1–22], where relaxation time procedures are essential. Thus, for normalized relaxation modulus $g(t) = G(t)/G_0$, we get a Fredholm-type integral equation:

$$g(t) = \int_{-\infty}^{\infty} w(M) k(t, M) dM. \tag{7}$$

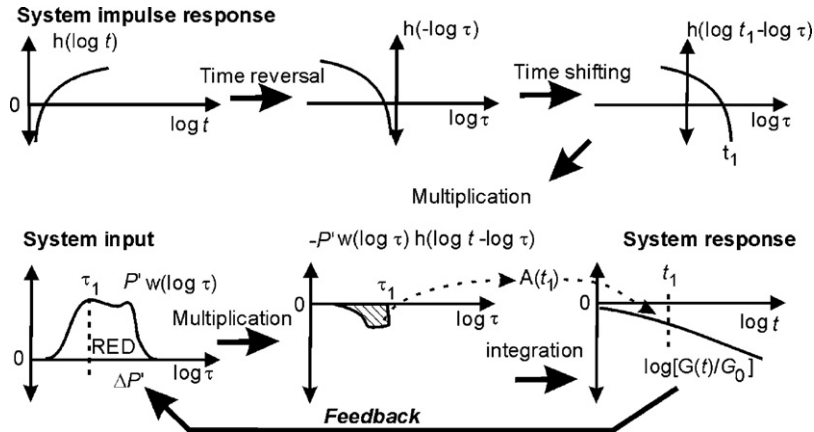


Fig. 1. Graphical demonstration of the system and polymer melt. The stress in the molecules decreases during relaxation in distribution $w(\log t)$, and the multiplication product must be negative. The response at time t_1 is defined by area $A(t_1)$, which is scaled by factor P' to obtain the system response as a normalized relaxation function $\log(G(t)/G_0)$. Precise modelling of system response $G(t)$ for the system input based on feedback information P' yields the correct RED function.

To aid the comparison, we rewrite Eq. (3) in a similar simplified style as

$$g(t) = \int_{-\infty}^t w(\tau)h(t - \tau)d\tau. \quad (8)$$

Both Eqs. (7) and (8) are known as convolution integrals, but the functional Eq. (8) has no relaxation time procedures or variables at different scales. Thus there are fundamental differences in relaxation times λ and their discrete spectra are artificial, whereas continuous distribution RED $w(t)$ is a true function in the form of statistical distribution for viscoelastic effects and MWD.

The form of the RED $w(\log t)$ function may be roughly similar to the relaxation time spectrum. In summary, there are essential and fundamental mathematical differences between the models, and the presented RED function $w(\log t)$ includes all types of chain dynamics.

2.2. Model for real polymer melts by the analytical model

Real polymer relaxation occurs in two phases: Rouse [27] relaxation, followed by entangled chain dynamics and reptation, primitive path fluctuations and constraint release. We refer to the second phase here as entanglement relaxation that exhibits mostly elastic effects and responses. Molecular entanglements will relax after deformation roughly at times $t > 0.001$ s, where most observations of $G(t)$ are made. Rouse theory starts from the molecular friction coefficient, where includes rapid elastic dumbbell effects that are mostly relaxed before melts are measured. We employ familiar terminology to introduce the principle of Rouse (viscous) and entanglement (elastic) relaxations, but as discussed in Section 2.1, the real chain dynamics are still open and both Rouse and entanglement relaxations have viscous and elastic components.

Since we have the same MWD acting for both Rouse relaxation and later for entanglement relaxation, we also use the entanglement distribution in common logarithm scale $w'(\log t)$ for the earlier effective Rouse distribution $w''(\log t_R)$, which corresponds to $w''(\log t - \log R) = w''(\log t/R)$ by standard time shifting. This is achieved simply by copying function $w'(\log t)$ after dividing t by the ratio, R , of the effective or “relaxation time” ranges. The distance for the same point for the effective Rouse and entanglement relaxations and the respective distribution, $w'(\log t)$, is $R = t_e/t_R$. Since Rouse relaxation occurs roughly at $t < 0.001$ s (which is outside the measurement range) and the form of the effective distribution has

a minimal effect on the obtained relaxation, the use of $w''(\log t/R)$ with a similar form is the best available choice without more information; nevertheless, the form of the w'' distribution can also differ. We use familiar viscoelastic notation since RED (or RED') $w'(\log t)$ and RED'' $w''(\log t/R)$ exhibit mainly elastic and viscous effects, respectively, in the observation range. We convert the relaxation formula of Eq. (5) to the entanglement and Rouse relaxation described by Eq. (9) and impulse response $\log t - \log \tau = \log(t/\tau)$.

In practice, the same distribution, $w'(\log t)$, is copied earlier to the timescale, and we obtain the following complete relaxation formula:

$$\log \frac{G(t)}{G_0} = - \int_{-\infty}^{\log t} \left(P'w'(\log \tau) + P''w''\left(\log \frac{\tau}{R}\right) \right) \log \frac{t}{\tau} d \log \tau, \quad (9)$$

where the scalar values are $0 < P' < 20$ for entanglement and $0 < P'' < 20$ for the Rouse relaxation ranges. The values of P' and P'' are not *ad hoc*, but are developed by the software during the procedure of fitting the relaxation modulus data and $w(t)$ distribution.

Eq. (9) models relaxation modulus $G(t)$ without difficulty, but solving distribution $w'(t)$ or functions with a logarithmic kernel is a severely ill-posed problem reported by Bruckner and Cheng [28]. Therefore, in Section 2.4 we present an alternative solution method.

2.3. Melt calibration

We need to convert distribution scales between molecular weight scale M and rheologically effective scale as a function of time t by introducing the *melt calibration*, which is the relation between rheological properties and the molecular weight.

A test point in a relaxed polymer melt after small deformation at t_0 can be approximated statistically as a nonrelaxed sphere of volume V_0 with an average molecular size up to $M(t_0)$. The apparent sphere of effective molecules starts to shrink as a function of radius $r(t)$, with those molecules located farthest from the test point relaxing first due to elastic effects or molecular and any types of chain dynamics such as reptation, primitive path fluctuations and constraint release in longitudinal modes. Molecules of any kind (as discussed in Section 2.1) that are farther from the test point deform less, as shown in Fig. 2a. The average molecular size inside the sphere is $M = Mf dV/V_0$, where Mf is the *polymer structural value* that depends on the molecular structure and weight. The effective volume for the nonrelaxed sphere and thus the effective molecular size change dM , as a function of $r(t)$, is given by $dM = Mf(4/3)\pi(d r^3/V_0)$, where $Hf = (4/3)\pi \approx 4.19$ is the *conversion factor* between scales M

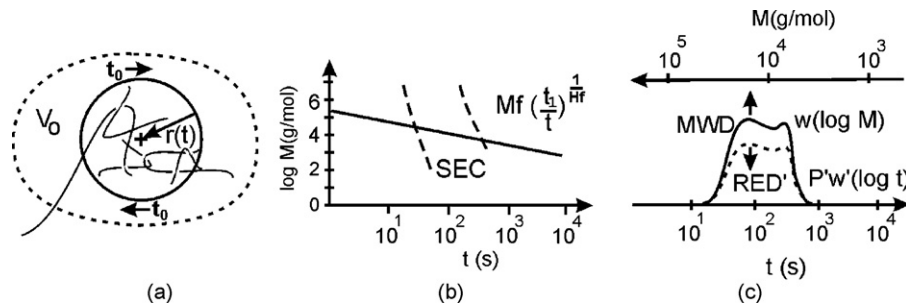


Fig. 2. Relation model for melts, and conversions from the RED to the MWD. (a) In a relaxed polymer, a test point in the melt after a small shear deformation at t_0 is equivalent to a statistical nonrelaxed sphere of volume V_0 , which shrinks as a function of radius $r(t)$ as the farthest molecules or the ends of individual molecules relax first, resulting in less deformation relative to the test point. (b) Melt calibration curve $M(t)$ for PS, and the respective typical universal calibration curves for different SEC columns marked by dashed lines. (c) RED $w'(\log t)$ from the timescale converted to inverse molecular weight scale w (top) and MWD $w(\log M)$ or $w(\log M) = w'(\log t)$ using Eq. (11).

and t . By induction, we can similarly model all the test points of the melt, where the distance to walls is greater as $r(t_0)$.

The relation between molecular weight scale M and rigid timescale t is obtained using a homogeneous linear differential formula. The additional decrease in dM converted by Hf on the M scale according to $-dM/dt$ must equal the molecular weight scale divided by time, M/t , or

$$Hf \frac{dM}{dt} + \frac{M}{t} = 0. \quad (10)$$

Solving Eq. (10) yields a simple relation for $t > 0$, which is the melt calibration, $M(t)$, as a function of time, where for the factor Mf value is M at $t_1 = 1$ s:

$$M = Mf \left(\frac{t}{t_1} \right)^{-(1/Hf)}. \quad (11)$$

For polymer measurements, the Hf conversion factor is usually close to 4, and Mf takes values between 10^2 and 10^6 g/mol. Benoit and co-workers [29] introduced the universal calibration concept for GPC (that was subsequently also applied to SEC), which used the hydrodynamic volume, and here the nonrelaxed melt volume is used. Fig. 2b shows the melt calibration curve for polystyrene (PS) and compares it to the SEC calibration.

We need to convert RED $w'(t)$ to MWD $w(M)$ or in logarithmic scales $w(\log M) = w'(\log t)$. When an effective distribution function $w'(\log t)$ is found from the best fit to the relaxation modulus, we can convert it by variable transformation to $w(\log M)$ using the standard as multivariate change-of-variables formula used with GPC/SEC, Eq. (11), and the exponent (i.e., conversion factor between scales Hf and the polymer structural value Mf results shown in Fig. 2c).

The correct value of the Mf factor for each polymer type is found from fitting GPC, SEC, absolute multiangle

light-scattering measurements, dynamic measurements, and models.

The response for RED $w'(t)$ of the different effective fractions is not linear, since different types of polymer mixtures or some complex molar structures can be involved, and hence we have to use a curve-fitting procedure similar to that used with universal calibration as presented in Fig. 2b. The two dashed nonlinear SEC calibration curves in the figure are found in practice after several analyses. It is noteworthy that the linear curve for LCB polyethylene (PE) is the same as that for the base MWD.

2.4. Effective distribution $w'(t)$ by the characteristic model

We have to extract effective distribution $w'(t)$ from Eq. (9), but attempting to do this directly leads to an ill-posed problem. Thus, to make the computations practical we use the faster and simpler characteristic model to obtain the form of the RED curve and MWD.

We first approximate the convolution integral in Eq. (9) as a summation, from which it is then possible to solve derivative $w'(t)$ directly by computation. Eq. (4) was previously converted to the logarithmic form for system response $y(\log t)$, which is actually the sum of impulse responses as a series of logarithmic time steps $\Delta \log T$ as a function of i items:

$$y(\log t) = \sum_{i=0}^{\infty} (w(i \Delta \log T) \Delta \log T) h(\log t - i \Delta \log T). \quad (12)$$

If we set $\Delta \log T \rightarrow 0$, this equation simplifies to the original convolution form shown in Eqs. (4) and (5). To obtain the sample or characteristic response $y_c(\log t)$ for characteristic relaxation

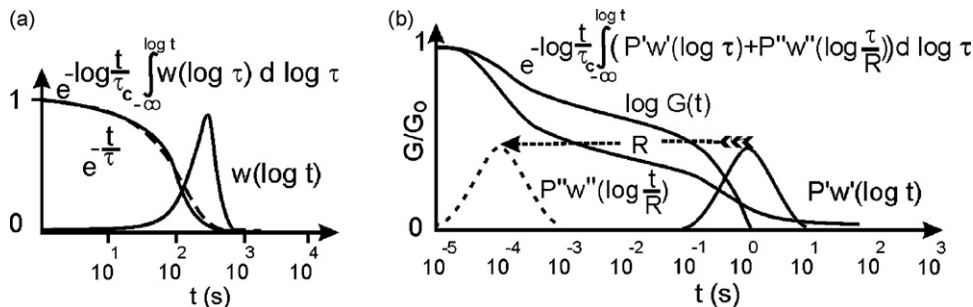


Fig. 3. Schematic models of the relaxation modulus. (a) The standard normal rheologically effective distribution (RED), $w'(t)$, plotted on a logarithmic scale with $\tau_c = 1$ s. Its characteristic relaxation is very close to the classical Maxwellian single-element relaxation, with $\lambda = 100$ s (dashed line). (b) Relaxation by Eq. (13) using the log-normal distributions $w(\log t)$ and $w''(\log t/R)$, with constants $\tau_c = 10^{-6}$ s, P' and P'' set completeness to 0.1, and $R = 10^4$. Both normalized relaxation moduli $G(t)/G_0$ and logarithmic $\log G(t)$ with illustrated $G_0 = 10$ Pa are shown. Typical similar real polymer has the average molecular weight \bar{M}_w in the range 100,000 g/mol, and the polydispersity index, M/M_n below 1.2.

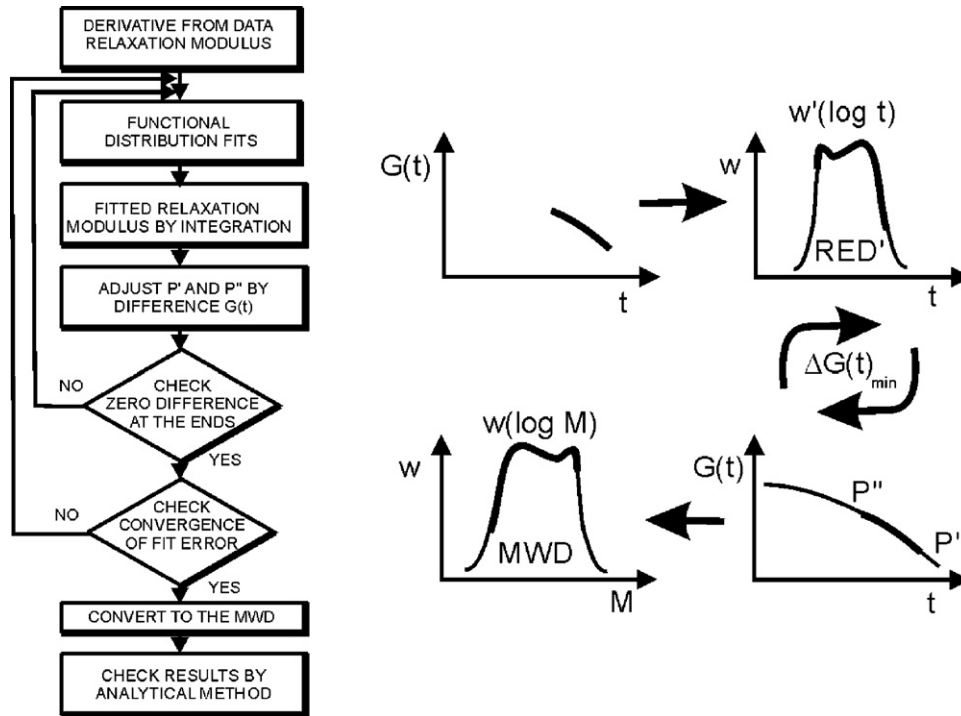


Fig. 4. Flowchart for the algorithm used to determine the MWD and the modelled relaxation modulus on a logarithmic scale and respective data flowchart of the procedure. Thick lines show derivative results, and thin lines are the results for the characteristic and analytical models. The best fit to $\Delta G(t)_{\min}$ is obtained by a standard numerical least-squares computation.

time τ_c , we set it equivalent to the shifted impulse response, or $i \Delta \log T = \log \tau_c$. The time-shifted impulse response is now converted to $\log t / \tau_c$, and the complete formula becomes a standard integral. See illustrations in Fig. 3. Thus, in analytical Eq. (9), relaxation modulus $G(t)$ can be approximated as a standard integral of the RED and we obtain characteristic relaxation modulus $G_c(t)$ for constant τ_c as

$$\log \frac{G_c(t)}{G_0} = - \log \frac{t}{\tau_c} \int_{-\infty}^{\log t} \left(P' w'(\log \tau) + P'' w'' \left(\log \frac{\tau}{R} \right) \right) d \log \tau. \quad (13)$$

The logarithmic impulse response has the greatest influence in this special case at time t_0 in Eqs. (4) and (12), where τ_c is also rather small, approaching $\Delta \log T$ at small values of index i . These points are most representative of the convolution and the relations from $w'(\log t)$ to $G(t)$ and $G_c(t)$, which we show in Section 3.3 to be within the measurement error. A novel idea is to use originally normalized $G(t)$ and $w'(t)$ distribution in both methods, for which the lack of absolute values do not cause difficulties.

This procedure removes the absolute value of the pulse response, but this is not a problem since we were originally using only relative values. The relaxation modulus obtained from this simple characteristic model is very close to that obtained from the analytical model shown in Fig. 5, and within the $G(t)$ measurement errors. Both the analytical and characteristic models have the same distribution $w'(t)$ giving the system response as relaxation modulus data $G(t)$. Of even more importance is that Eq. (13) can be solved for apparent and characteristic effective distribution $w'_c(t)$ simply by deriving as follows from the measured $G(t)$ to accurately obtain the shape of the RED curve:

$$w'_c(\log t) = - \frac{d}{d \log t} \frac{1}{P'} \left(\frac{\log(G(t)/G_0)}{\log(t/\tau_c)} + P'' \int_{-\infty}^{\log t} w''(\log(\tau/R)) d \log \tau \right). \quad (14)$$

Normally, distribution $w'(\log t)$ and its copy $w''(\log t/R)$ have zero or minimal overlap. The effective distribution can be computed over several iterations to find the best fit between the measured and modelled viscosities. During each derivation, the Rouse distribution $w''(\log t/R)$ can be assumed to be constant, and a new form is refreshed with a new $w'(\log t)$ for each iteration. The RED curve is precisely obtained from Eq. (14) in the measurement range using direct numerical differentiation.

Now we can again model $G(t)$ according to analytical formula Eq. (9) using the obtained RED and even attempt to solve $w'(\log t)$ with regularization methods and the aid of a priori knowledge. Since this analytical method requires considerable computation time and the obtained RED curve is not accurate, we only present results for the characteristic model; however, both models can complement each other in simultaneous parallel computing.

The P' and P'' values differ between the analytical Eq. (9) and characteristic Eq. (13) model, but their values are easily found by computation (Fig. 4).

In summary, we first apply a rapid integration method based on derivatives for the time-consuming cyclic computation. The relation between MWD and measurements obtained using the characteristic method is then confirmed using the analytical method. These two methods are complementary, and can be used in parallel computing.

2.5. Relaxation modulus level from viscosity data

In cases where we are using only viscosity data, we do not obtain the absolute level of the relaxation modulus directly. Since we simultaneously obtain the zero viscosity (η_0) using a wide-range viscosity fit and the normalized relaxation modulus, $g(t) = G(t)/G_0$, we need tools to find an absolute value for G_0 . Here we can use standard simple numerical fitting procedures such as bracketing, while solving Eq. (13) by testing with new \hat{G}_0 values to obtain the new $G_0 = \hat{G}_0$.

$$\eta_0 = \int_{-\infty}^{\infty} t \hat{G}_0 g(t) dt \log t. \tag{15}$$

An alternative, simpler procedure can be used if we know even a single data point in the measured relaxation modulus curve $G(t)$ and MWD with known constants.

2.6. Assumptions and limitations

In principle, relaxation modulus $G(t)$ data are suitable as a data source, but have been found to be of limited use in computations due to distortion resulting from procedural and instrumental sources. During experiments, some deformation always occurs before relaxation. The simulation is at best a two-step process, because earlier states and deformation histories considerably influence the measured properties. Inertial forces of the oscillating head of the device also cause visible errors in the $G(t)$ data. However, very recently there have been promising developments in rotational rheometers to obtain more accurate $G(t)$ data.

Whilst developing the principle, we found that the relation between the measured storage $G'(\omega)$ and loss modulus $G''(\omega)$ does not fit accurately in principle, with only the complex modulus $G^*(\omega)$ being reliable. This explains why there is no widely used regularized method for generating the relaxation modulus, $G(t)$. Moreover, no developed master curves or conversions give direct and accurate experimental data for analysis.

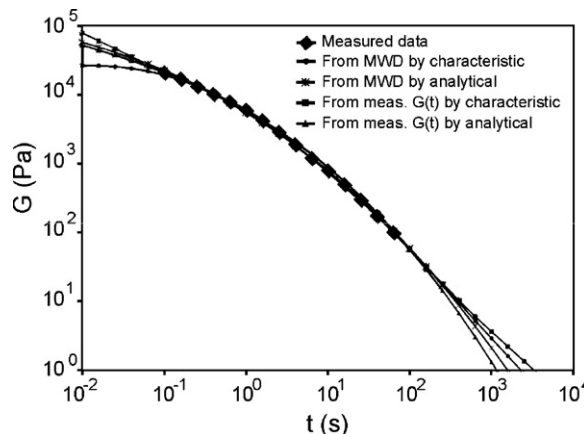


Fig. 5. Relaxation modulus for IUPAC A LDPE in the range of measurements performed by Meissner [30] from 0.1 s only up to 80 s at 150 °C. Both analytical Eq. (7) and the derived characteristic equation (Eq. (13)) show minimal differences between the models over the measurable range shown with larger markers, and are virtually indistinguishable.

The glassy modulus relaxes within 10^{-11} s, which can be modelled easily by adding to Eqs. (9) and (13) the third RED''' distribution $P''' w'''(t)$ close to the same time period.

3. Experiments

3.1. Procedure and test polymers

All the computations described here were performed on a standard PC using RheoPower software and the characteristic model described by Eqs. (13) and (14), except for Fig. 5, which also used the analytical model. A data record is first imported into the databases, the Mf and Hf constants are selected, and then the programs are run on the PC. It is well known that detecting the MWD and

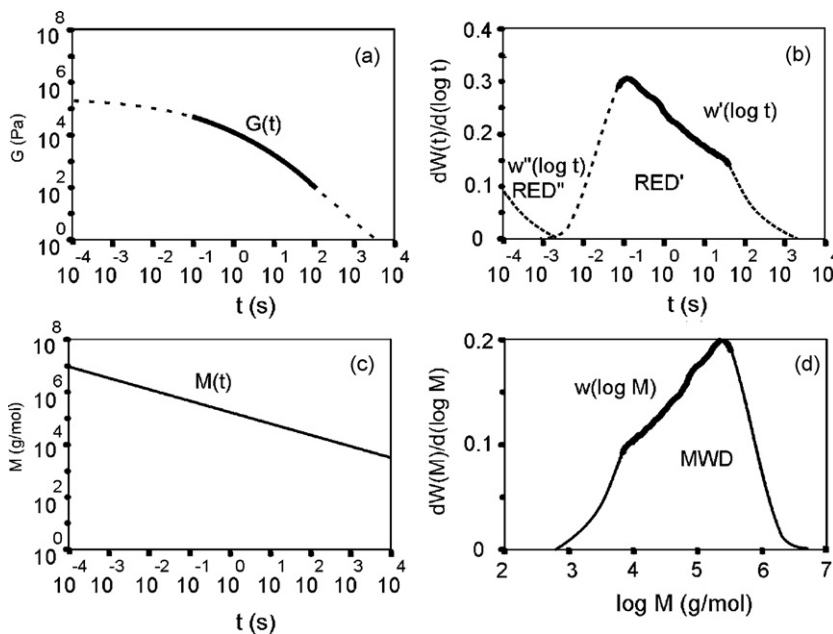


Fig. 6. From relaxation modulus to MWD of IUPAC A LDPE at 150 °C. (a) Thicker segment of measured relaxation modulus $G(t)$ and wider thin dashed curve generated by modelling from complete $w(t)$ of (b) using Eq. (13). (b) Thicker segment of the curve of the rheologically effective distribution (RED), $w(t)$, was computed directly from measured relaxation modulus $G(t)$ using Eq. (14), and thinner dashed segment was obtained by applying a standard best-fit procedure between measured and modelled $G(t)$ as in (a). (c) Melt calibration curve $M(t)$ according to Eq. (11) transforms $w(t)$ to MWD $w(\log M)$. (d) The MWD is converted from RED function in (b) in a manner similar to GPC/SEC techniques. It is now possible to analytical compute $G(t)$ backwards from the obtained MWD so as to check the accuracy of the analysis results.

modelling the rheology is most difficult for polyolefins among all polymers.

LDPE IUPAC A low-density polyethylene (LDPE) was adopted as the LDPE sample since measured data are available and this material has been used in many other studies or “Melt I”, first published by Meissner [30].

3.2. Constants

The default value of $R = 10^6$ for distance was set for the Rouse shear range distribution except for Fig. 3 was used $R = 10^5$. For the LDPE sample, $M_f = 37,800$ g/mol at 150°C was used. The relation scale exponent for PE, $H_f = 2.05$, was taken as constant for polyolefin with a plate–plate oscillating rheometer. It must be noted that $H_f = 2.5$ represents the use of a cone–plate head, and that the value for PE has increased recently thanks to developments in GPC/SEC and viscoelastic measurements. For comparison, the respective constants for PS were $M_f = 136,000$ g/mol and $H_f = 4$, as commonly used for all other polymers except above polyolefin. Please note that the values P' and P'' were developed by the $G(t)$ fitting procedure and no *ad hoc* constants or values were used.

A constant characteristic time of $\tau_c = 10^{-6}$ s was used in the relaxation simulations.

3.3. Modelling relaxation modulus

We wanted to use the relaxation data measured at 150°C for IUPAC A as obtained manually from the sources stated by Meissner [30–32]. For this we drew an MWD curve by eye in RheoDeveloper (RheoPower) to provide a curve close to the original relaxation modulus curve. The average molecular weight \bar{M}_w for this LDPE was measured originally to be 472,000 g/mol, and the polydispersity index, M/M_n , was 24.9. We therefore used $\bar{M}_w = 480,000$ g/mol and $M/M_n = 25$ in our modelling.

The data for LDPE are collected in Fig. 5, which shows the relaxation modulus measured by Meissner [30] at 150°C and computed for IUPAC A. The figure indicates that the five relaxation curves are very similar (where the appropriate information is available). The MWD as measured by GPC was drawn using RheoDeveloper, and the relaxation modulus was computed using both analytical Eq. (9) and characteristic Eq. (13) models. The last two curves that used $G(t)$ data were measured by RheoAnalyzer, which developed internally the MWD or the better RED, and this distribution was used to model backward to get wide $G(t)$ fit curve. The wide scales of the relaxation modulus curve at 150°C computed using the integration formula and the MWD are shown in Fig. 6a.

4. Conclusions

A new method for modelling linear viscoelasticity and polymer properties is presented here, which is mathematically based on the control theory and on the concept of relations for melts and molecular weight fractions. Here the method has been used to determine the MWD from viscoelastic data and vice versa, providing a novel solution to this known ill-posed problem that shows that the MWD can be obtained directly by derivation. Complete linear viscoelastic relaxation involves chain dynamics, since the initial Rouse relaxation according to the RED gives only a viscous response in the measurement range, whereas the mainly elastic RED is affected by entanglement relaxation. Since these REDs exhibit only minimal overlap on the relaxation timescale, it is possible to extract the RED and further the MWD by melt calibration. This generates an accurate viscoelastic relaxation modulus, although it is composed from two separate viscoelastic REDs.

We are currently improving the analytical model, performing simultaneous parallel computations, and comparing the results between analytical and characteristic models. The major known limitation of our method is that relaxation modulus is difficult to measure directly, with the use of complex viscosity data in the procedure giving a much more accurate MWD and other results. Further results with a deeper explanation and more polymer types, and a description of the numerical methodology of the procedure are available elsewhere by Borg and Pääkkönen [32]. In short, our procedure is more understandable from the viewpoint of $G(t)$. Whilst the principle underlying our procedure is simple, the numerically sensitive and labile recursive exponential formulas require the use of accurate data with specialized software to achieve high computing accuracy.

Acknowledgments

We thank for comments and support Dr. R.S. Anderssen from CSIRO on using the impulse function and Dr. Tech. K. Zenger from HUT on using the control theory, which considerably improved our paper.

References

- [1] C. Tsenoglou, Viscoelasticity of binary homopolymer blends, ACS Polym. Prepr. 28 (1987) 185–186.
- [2] J. Des Cloizeaux, Double reptation vs simple reptation in polymer melts, Europhys. Lett. 5 (1988) 437–442, 6 (1988) 475; Erratum, Europhys. Lett. (1988), 475; J. Des Cloizeaux, Double reptation vs simple reptation in polymer melts, Europhys. Lett. 6 (1988) 475.
- [3] S.H. Wasserman, W.W. Graessley, Effects of polydispersity on linear viscoelasticity in entangled polymer melts, J. Rheol. 36 (1992) 543–572.
- [4] P. Cassagnau, J.P. Montfort, G. Marin, P. Monge, Rheology of polydisperse polymers; relationship between intermolecular interactions and molecular weight distribution, Rheol. Acta 32 (1993) 156–167.
- [5] H. Mavridis, R.J. Shroff, Appraisal of a molecular weight distribution-to-rheology conversion scheme for linear polyethylenes, J. Appl. Polym. Sci. 49 (1993) 299–318.
- [6] D.W. Mead, Determination of molecular weight distributions of linear flexible polymers from linear viscoelastic material functions, J. Rheol. 38 (1994) 1797–1827.
- [7] S.H. Wasserman, Calculating the molecular weight distribution from linear viscoelastic response of polymer melts, J. Rheol. 39 (1995) 601–625.
- [8] S.H. Wasserman, W.W. Graessley, Prediction of linear viscoelastic response for entangled polyolefin melts from molecular weight distribution, Polym. Eng. Sci. 36 (1996) 852–861.
- [9] M.R. Nobile, F. Cocchini, J.V. Lawler, On the stability of molecular weight distributions as computed from the flow curves of polymer melts, J. Rheol. 40 (1996) 363–382.
- [10] D. Maier, A. Eckstein, C. Friedrich, J. Honerkamp, Evaluation of models combining rheological data with the molecular weight distribution, J. Rheol. 42 (1998) 1153–1173.
- [11] F. Léonardi, A. Allal, G. Marin, Determination of the molecular weight distribution of linear polymers by inversion of a blending law on complex viscosities, Rheol. Acta 37 (1998) 199–213.
- [12] W. Thimm, C. Friedrich, M. Marth, J. Honerkamp, An analytical relation between relaxation time spectrum and molecular weight distribution, J. Rheol. 43 (1999) 1663–1672.
- [13] W. Thimm, C. Friedrich, M. Marth, J. Honerkamp, On the Rouse spectrum and the determination of the molecular weight distribution from rheological data, J. Rheol. 44 (2000) 429–438.
- [14] E. van Ruymbeke, R. Keunings, C. Bailly, Determination of the molecular weight distribution of entangled linear polymers from linear viscoelasticity data, J. Non-Newtonian Fluid Mech. 105 (2002) 153–175.
- [15] F. Léonardi, A. Allal, G. Marin, Molecular weight distribution from viscoelastic data: the importance of tube renewal and Rouse modes, J. Rheol. 46 (2002) 209–224.
- [16] E. van Ruymbeke, R. Keunings, V. Stéphenne, A. Hagenaaers, C. Bailly, Evaluation of reptation models for predicting the linear viscoelastic properties of entangled linear polymers, Macromolecules 35 (2002) 2689–2699.
- [17] F. Cocchini, M.R. Nobile, Constrained inversion of rheological data to molecular weight distribution for polymer melts, Rheol. Acta 42 (2003) 232–242.
- [18] J.F. Vega, S. Rastogi, G.W.M. Peters, H.E.H. Meijer, Rheology and reptation of linear polymers. Ultrahigh molecular weight chain dynamics in the melt, J. Rheol. 48 (2004) 663–678.

- [19] M.R. Nobile, F. Cocchini, A generalized relation between MWD and relaxation time spectrum, *Rheol. Acta* 47 (2008) 509–519.
- [20] J.D. Guzmán, J.D. Scieber, R. Polland, A regularization-free method for the calculation of molecular weight distributions from dynamic moduli data, *Rheol. Acta* 44 (2005) 342–351.
- [21] C. Pattamaprom, R.G. Larson, A. Sirivat, Determining polymer molecular weight distributions from rheological properties using the dual-constraint model, *Rheol. Acta* 47 (2008) 1435–1528.
- [22] R.S. Anderssen, D.W. Mead, Theoretical derivation of molecular weight scaling for rheological parameters, *J. Non-Newtonian Fluid Mech.* 76 (1998) 299–306.
- [23] W.W. Graessley, *Polymeric Liquids and Networks: Dynamics and Rheology*, Garland Science, London, 2008.
- [24] R.S. Anderssen, R.J. Loy, On the scaling of molecular weight distribution functionals, *J. Rheol.* 45 (2001) 891–901.
- [25] R.S. Anderssen, R.J. Loy, Rheological implications of completely monotone fading memory, *J. Rheol.* 46 (2002) 1459–1472.
- [26] S. Matsuoka, *Relaxation Phenomena in Polymers*, Hanser, Munich, 1992.
- [27] P.R. Rouse Jr., A theory of the linear viscoelastic properties of dilute solutions of coiling polymers, *J. Chem. Phys.* 21 (1953) 1272–1280.
- [28] G. Bruckner, J. Cheng, Tikhonov regularization for an integral equation of the first kind with logarithmic kernel, *J. Inverse Ill-posed Problems* 8 (2000) 665–675.
- [29] Z. Grubisic, P. Rempp, H. Benoit, A universal calibration for gel permeation chromatography, *Polym. Lett.* 5 (1967) 753–759.
- [30] J. Meissner, Basic parameters, melt rheology, processing and end-use properties of three similar low-density polyethylene samples, *Pure Appl. Chem.* 42 (1975) 551–662.
- [31] J. Meissner, Modifications of the Weissenberg Rheogoniometer for measurement of transient rheological properties of molten polyethylene under shear. Comparison with tensile data, *J. Appl. Polymer Sci.* 16 (1972) 2877–2899.
- [32] T. Borg, E.J. Pääkkönen, Linear Viscoelastic Models, *J. Non-Newtonian Fluid Mech.* (2008), doi:10.1016/j.jnnfm.2008.07.010.